Optical Measurement of Wall Shear Stress With Emphasis on Flows Near Separation

D. Fourguette, P. Gonzalez, D. Modarress, E. Arik, D. Wilson[#], M. Koochesfahani*

VioSense Corporation
36 S. Chester Ave., Pasadena, CA 91106

24th AIAA Aerodynamic Measurement Technology and Ground Testing Conference
28 June-1 July 2004
Portland, OR

Abstract

We describe a new generation of a MEMS based optical microsensor, the Diverging Fringe Doppler sensor, designed to measure the flow velocity gradient within the first 100 μm of a surface. The sensor measures the flow velocity gradient at 75 μm above the sensor surface as well as flow direction. This compact and embeddable sensor uses diffractive optical elements to generate diverging fringes originating at the sensor surface and slanted at 20° from the normal to the sensor face. The slant introduced in the fringes is used to measure flow directionality. The sensor was tested in the boundary layer of a flat plate. Subsequently, the sensor was installed in a cylinder and tested in the boundary layer of that cylinder from the stagnation point to the separation region of the flow, for Reynolds numbers of 10^4 and 4 x 10^4. In both cases, the results were compared to that obtained with a miniature laser Doppler velocimeter mounted on a traverse, also embedded into the cylinder. The design of the sensor and instrumentation, and the experimental results are presented in this paper.

Introduction

Wall shear stress sensors (an exhaustive review of shear stress measurement techniques is provided in Reference 1 and Reference 2) calculate the shear stress from measurements performed at the surface, mechanically using a floating element or thermally using heat dissipation, or infer the shear stress at the wall from velocity measurements performed within the viscous sub-layer of the boundary layer. A workshop[3] on shear stress measurement techniques was held at the California Institute of Technology in February 2004[&]. Presently, no wall shear stress measurement approach is free and clear of significant limitations. Surface mounted thermal sensors suffer from heat transfer problems, thus making an accurate calibration a difficult task while velocity measurements are limited to relatively low Reynolds numbers because of the requirement for the measurement to be located within the linear sub-layer, $y^+<5$. The optical sensor described here uses a technique developed by Naqwi and Reynolds[4] who measured the velocity gradient within the first hundred microns above the wall using a diverging fringe pattern originating at the wall. In that arrangement, the velocity and the fringe spacing increase proportionally with the distance from the wall. This technique has been shown to yield accurate measurements[5] of the velocity

[&] Proceedings (CD format) is available upon request from the third Author.

Jet Propulsion Laboratory, Pasadena, CA
* Michigan State University, East Lansing, MI

gradient at the wall for Reynolds numbers of up to 10^8.

The Diverging Fringe Doppler sensor described here is designed and fabricated using MOEMS (Optical MEMS), i.e., computer generated holographic elements or diffractive optical elements (DOE)[6-8]. Diffractive optical elements are unique in the sense that complex optical probe volume geometries, otherwise difficult or impossible to achieve using conventional optics, can be precisely positioned in space. The diffractive elements used in this application are square shaped not larger than 500 μm on the side. This technology enables the development of very compact, embeddable sensors. These compact sensors can then be embedded into models, and maintain a fixed working distance throughout the tests. The miniature laser Doppler velocimeter (MiniLDV) used for this experiment was specially designed using optical MEMS and conventional optics to fit inside the 4" diameter test cylinder. The miniature LDV was frequency shifted to measure velocity near flow separation conditions.

The combined results from the miniature LDV mounted on a traverse and two versions of the Diverging Fringe Doppler sensor are presented here. The measurements were conducted in the boundary layer of a flat plate and in the boundary layer of a cylinder in a cross flow. A good agreement was found between the shear stress values calculated from the velocity gradient measured with the Diverging Fringe Doppler sensor and the predicted values using the Thwaites method. The boundary layer surveys obtained with the MiniLDV produce lower estimates for the shear stress. Several reasons for this behavior are suggested later in this paper. The Diverging Fringe Doppler sensor was tested in forward and reverse flow conditions and demonstrated a 96% reliability in detecting the flow direction.

The Diverging Fringe Doppler sensor

Principle of operation

Figure 1 shows a schematic of the measurement principle. Diverging interference fringes originate at the surface and extend into the flow. The scattered light from the particle passing through the fringes is collected through a window at the surface of the sensor. The region defined by the intersection of the transmitter and receiver fields was centered at approximately 75 μm above the surface and measured about 30 μm high.

The local fringe separation, δ, was designed to be linear with the distance from the sensor, y, given by $\delta = k \times y$, where k is the fringe divergence rate along the normal to the sensor surface. As particles in the fluid flow through the linearly diverging fringes, they scatter light with a frequency f that is proportional to the instantaneous velocity and inversely proportional to the fringe separation at the location of particle trajectory as shown in Figure 1. The velocity of the particle is therefore $u = f \times \delta$. The Doppler frequency simply multiplied by the fringe divergence yields

$$\frac{u}{y} = f \times k \quad (1)$$

which is equal to the wall velocity gradient, , assuming that the probe volume is located within the laminar sub-layer of the boundary layer. The wall shear is then calculated from the following relationship.

$$\sigma = \mu \frac{\partial u}{\partial y}\Big|_w \equiv \mu \frac{u}{y} \quad (2) .$$

The signal conditioning and processing required for the diverging fringe optical sensor described here is identical to those used for the LDV instrument.

A schematic of the optical MEMS sensor is shown in Figure 2. The light output from a single mode fiber illuminates the transmitter DOE to focus the light into two elongated

spots which pass through slits etched into a chrome mask. The cylindrical wave fronts emerging from the slits form a fringe pattern 20 μm above the sensor surface. Particles contained in the flow travel through the fringe pattern, thus generating a burst similar to that recorded with an LDV. The scattered light collected through a window etched in the chrome mask is focused onto a multimode fiber connected to an avalanche photodiode for photonic conversion. Figure 3 shows a photograph of the Diverging Fringe Doppler sensor.

Directionality

The fringes generated by the Diverging Doppler sensor were slanted at 20^o from the normal to the sensor face, as sketched in Figure 2. The optical simulation conducted to generate the slant in the fringes is shown in Figure 4. The orientation of the fringe line optimized the sensor's collecting lens efficiency and provided directionality in the output signal. A particle traveling along a trajectory parallel to the sensor will experience an increasing fringe spacing traveling from left to right and inversely, a decreasing fringe spacing traveling from right to left.

As an example, two bursts are shown in Figure 5, where the decreasing frequency is visible in the case of fringes slanted away from the flow and increasing where fringes are slanted toward the flow.

A simple algorithm was written to measure the locations of the maximum amplitude of the signal, thus providing the period of successive cycles. The rate of change between the cycles provided the particle motion direction, and therefore the flow direction with respect to the sensor.

The Miniature LDV

The miniature LDV developed by VioSense was designed with both conventional and optical MEMS components[9]. While the sensor can be designed for a working distance as large as 500 mm, the LDV designed for the boundary layer surveys was equipped with a short working distance of 50 mm, to maintain a short probe volume length. The MiniLDV was attached to a traversing stage and all positioned inside the cylinder. The probe volume was traversed across the boundary layer thorough a right angle mirror and a transparent cylindrical window flush mounted with the cylinder.

Results

Measurements on a laminar flat plate boundary layer

Preliminary tests of the diverging Doppler sensor were conducted in a free surface water tunnel facility at the Graduate Aeronautics Laboratory of the California Institute of Technology. The facility was equipped with a 90 cm long test section in which different model geometries can be inserted. A flat plate was positioned on the free surface of the tunnel. The diverging Doppler sensor and the miniature LDV were mounted at 27.9 cm and 35.0 cm from the leading edge respectively.

A schematic of the experimental setup is shown in Figure 6 and a photograph is shown in Figure 7. The diverging Doppler sensor embedded in the flat plate is visible in front of the LDV mounted on the traverse.

Measurements were made at free-stream velocities of U_0=12 cm/s and U_0=18 cm/s. Velocity surveys were conducted in the boundary layer with a miniature LDV equipped with a working distance of 50 mm. The probe volume dimensions of the LDV were approximately 40 x 60 x 100 μm^3.

A Blasius fit was applied to the boundary layer profiles and compared to the results obtained at a fixed position with the two versions of the Diverging Fringe Doppler sensor, MicroS3-V11-1.5 with 1.5 μm slit width and MicroS3-V11-1.75 with 1.75 μm slit width. The comparison between the results obtained with the MiniLDV and the Diverging Fringe Doppler Sensors is shown in Figure 8.

These results show that the measurements obtained with both Diverging Fringe Doppler sensors mutually agree and also agree well

with those obtained from the boundary layer surveys conducted with the LDV.

Test with flow past a cylinder

A cylinder 100 mm in diameter was specially designed to receive an embedded traversing LDV and two diverging Doppler sensors. A mechanical design of the apparatus is shown in Figure 9. The design on the left shows the cylinder with the miniature LDV and diverging Doppler sensors (MicroS[3] in the drawing). The miniature LDV was specially designed such that the optical path for both the transmitter and the receiver was at right angle from the sensor body. In that configuration, the axis of the sensor was parallel to the axis of the cylinder. The LDV was mounted on a traverse for accurate survey of the boundary.

Figure 10 shows a photograph of the instrumented cylinder. The LDV body is visible installed along the cylinder length. One Diverging Fringe Doppler sensor is installed in one of the ports. A contoured lid comes over the opening to close the cylinder body with a watertight seal.

The cylinder was mounted on a rotation stage, suspended from a frame. The frame was designed to rest on the tunnel walls, supporting the cylinder such that a minimum clearance was left between the cylinder and the bottom surface of the tunnel. Tests were conducted in two different free surface tunnels at the California Institute of Technology, the "Noah Tunnel" and the "Large Free Surface Tunnel".

Tests in the Noah Tunnel

After preliminary tests to verify the proper functioning of the instrumentation, the cylinder was installed in the Noah water tunnel. The location and dimensions are shown in Figure 11. A photograph of the cylinder installed in the Noah tunnel is shown in Figure 12. The frame resting on the tunnel walls and holding the cylinder in the tunnel and the rotation stage are visible at the top of the photograph. The cylinder was equipped with a glass section visible at the bottom of the cylinder for future PIV measurements.

This series of tests was intended to verify the performance of the entire setup. Boundary layer surveys and velocity gradient measurements were obtained with the LDV and a Diverging Fringe Doppler sensor respectively for different azimuthal angles. The velocity gradient at the wall was calculated from the boundary layer surveys by fitting a line through the last few point measurements (5 points) closest to the wall. This method of estimating the gradient does not include the effects of pressure gradients in the flow and work is underway to develop a proper fitting method to the LDV data.

The normalized shear stress was calculated from the measurements. The results are shown in Figure 13. The solid curve represents the theoretical value of the shear stress calculated using the velocity distribution around the cylinder obtained using the Thwaites method[10].

The shear stress results show a good agreement with the theoretical curve. The values of shear stress obtained from the LDV data show a bias toward lower values. This finding can be explained by several observations. Previous measurements in the boundary layer of a flat plate[11,12] showed that a weak favorable pressure gradient is sufficient to bias the calculations of the velocity gradient at the wall toward lower values. The results shown in this figure do not take this effect into account. In addition, measurements with a finite size probe volume will spatially low-pass filter velocity measurements in a boundary layer, thus yielding a smaller calculated shear stress value.

Tests in the Large Free Surface Tunnel

The cylinder was positioned in the test section of the Large Free Surface Tunnel. The position of the cylinder is shown in Figure 14 and a photograph is shown in Figure 15. The LDV output is visible as the red beams in the photograph.

As in the Noah tunnel test, boundary layer surveys and velocity gradient measurements

were obtained with the LDV and the Diverging Fringe Doppler sensor respectively for different azimuthal angles. The normalized shear stress was calculated from the measurements. The results obtained for angles between -80^o to 80^o are shown in Figure 16. The values of the shear stress obtained with the Diverging Fringe Doppler sensor agree well with the predicted values obtained with the Thwaites method. The shear stress values obtained with the sensors mutually agree for the free stream velocity of approximately 10 cm/s but are slightly higher than the predicted value. We believe that the discrepancy can be attributed to the accuracy with which the free stream velocity was determined. Again, smaller shear stress estimates are obtained using the LDV surveys, for the same reasons as described for the tests in the Noah tunnel.

To verify the symmetry between both azimuthal directions, the results were folded onto one axis, from 0^o to 80^o. The solid curve represents the theoretical value of the shear stress calculated using the velocity distribution around the cylinder obtained by the Thwaites method. The results are shown in Figure 17.

The negative shear stress measurements shown in Figure 17 indicate that the velocity gradient measurements showed an opposite sign and therefore flow reversal after separation. This result shows that the Diverging Fringe Doppler sensor is capable of detecting flow directionality. A test was conducted to assess the reliability of the sensor in detecting flow reversal.

Directionality

Since the Diverging Fringe Doppler sensor generates fringes slanted from the normal, velocity gradient measurements were collected with the fringes facing away from the flow (A) and into the incoming flow (B). This was achieved by rotating the cylinder into position as shown in Figure 18.

The azimuthal angle was set such that the sensor was always well upstream of the separation point in each case, therefore all the records for each set were guaranteed to show the same frequency change within each burst. For each data set, the change of frequency was calculated within each burst. Figure 19 shows the probability of an experimental measurement to run in the positive direction for different angles. The sensor correctly measured the directionality of particles on the interval from 0 to +80° within a 96% confidence. The point to the left of the graph accurately indicates a flow reversal past the separation region.

On the interval from 0 to –80° there is a 4% probability of particles going in the positive direction (and thus a 96% in the negative direction) so the sensor also measured the correct known direction of the flow.

Conclusions

Recent progress in the development of a Diverging Doppler Fringe sensor was described. Boundary layer surveys and velocity gradient measurements with the Diverging Fringe Doppler sensor were conducted for both a flat plate boundary layer and the boundary layer of a flow past a cylinder. The cylinder was designed to house the Diverging Fringe Doppler sensor and a specially designed miniature LDV mounted on a traverse. The shear stress calculations based on the velocity gradient measurements at the wall with the Diverging Fringe Doppler sensor show good agreement with the predicted values based on the Thwaites method. The calculated shear stress values obtained from the boundary layer surveys are biased towards smaller shear stress values, which can be explained by the presence of a favorable pressure gradient and by the potential low pass filtering of the measurement technique. The Diverging Fringe Doppler sensor was capable of yielding flow direction with an accuracy of 96%. Additional work is underway to extend the measurements beyond the separation point and include the effects of pressure gradients in the fits of the boundary layer surveys.

Acknowledgements

The authors wish to acknowledge the useful discussions with Dr. Ki-Han Kim, Dr. David

Hess and Dr. P. Atsavapranee of ONR. The reported research was supported by ONR, under the Grant number N00014-03-C-0375.

References

1. Naughton, J.W., Sheplak, M., "Modern developments in shear stress measurements," Progress in Aerospace Sciences, 38 (2002).

2. Haritonidis, J.H., "The measurement of wall shear stress," in Advances in Fluid Mechanics, M. Gad-El-Hak (ed), Springer-Verlag (1989).

3. Proceedings of the Workshop in Shear Stress Measurement Techniques, California Institute of Technology.

4. Naqwi, A. A., Reynolds, W.C., (1987) "Dual cylindrical wave laser-Doppler method for measurement of skin friction in fluid flow," Report No. TF-28, Stanford University.

5. Fourguette, D., Modarress, D., Wilson, D., Koochesfahani, M., Gharib, M., "An Optical MEMS-based Shear Stress Sensor for High Reynolds Number Applications," 41st AIAA Aerospace Sciences Meeting and Exhibit, Reno, NV (2003).

6. D. W. Wilson, J. A. Scalf, S. Forouhar, R. E. Muller, F. Taugwalder, M. Gharib, D. Fourguette, and D. Modarress, "Diffractive optic fluid shear stress sensor," in *Diffractive Optics and Micro Optics*, OSA Technical Digest (Optical Society of America, Washington DC, 2000), pp. 306-308.

7. D. W. Wilson, P. K. Gogna, R. J. Chacon, R. E. Muller, D. Fourguette, D. Modarress, F. Taugwalder, P. Svitek, M. Gharib, "Diffractive Optics for Particle Velocimetry and Sizing" in Diffractive Optics and Micro Optics, OSA Technical Digest (Optical Society of America, Washington DC, 2002), pp. 11-13.

8. D. W. Wilson, P. D. Maker, R. E. Muller, P. Mouroulis, and J. Backlund, "Recent Advances in Blazed Grating Fabrication by Electron-beam Lithography," Paper 5173-16, Proc. SPIE (2003).

9. D. Modarress, D. Fourguette, F. Taugwalder, M. Gharib, S. Forouhar, D. Wilson, J. Scalf, "Design and Development of Miniature and Micro Doppler Sensors," 10th International Symposium on Application of Laser Techniques to Fluid Mechanics, Lisbon, Portugal (2000).

10. White, F. M., "*Viscous Fluid Flows*", McGraw Hill Publishing Company (1974).

11. M. Koochesfahani, D. Fourguette, D. Modarress, D. Wilson, "Experimental Evaluation of a Micro Optical Shear Stress Sensor," 54th APS/DFD Meeting, San Diego, CA (2001).

12. Fourguette, D., Modarress, D., Taugwalder, F., Wilson, D., Koochesfahani, M., Gharib, M., "Miniature and MOEMS flow sensors," 31st AIAA Fluid Dynamics Conference and Exhibit, Anaheim, CA (2001).

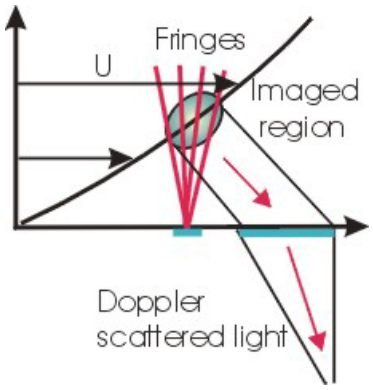

Figure 1. Schematic of the Diverging Fringe Doppler sensor principle of measurement.

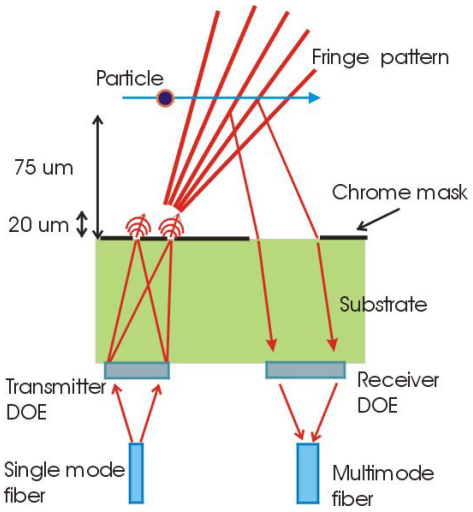

Figure 2 Schematic of the MOEMS sensor

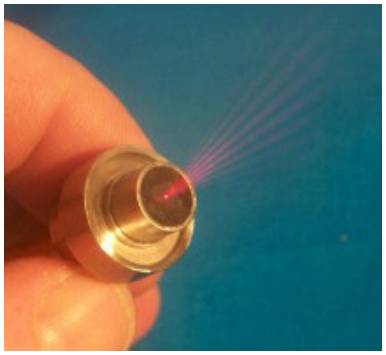

Figure 3 Photograph of the Diverging Fringe Doppler sensor

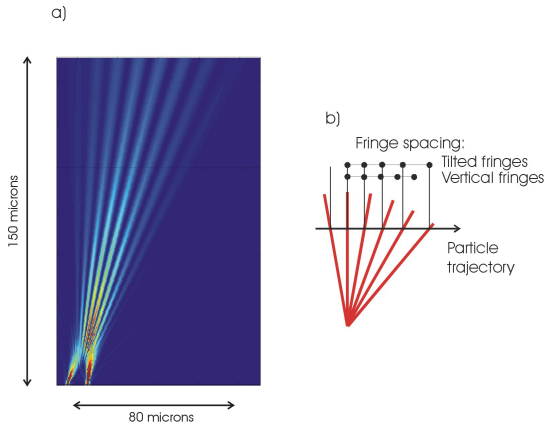

Figure 4 a) Simulation of the diverging optical fringe pattern generated by the Diverging Doppler sensor. The fringes are slanted at 20° from the normal to the sensor face. b) Schematic of the varying fringe spacing seen by a particle on a horizontal trajectory

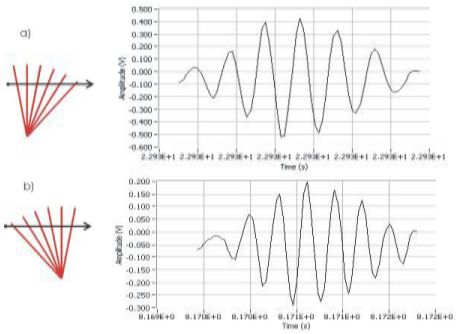

Figure 5 Bursts obtained with fringes slanted a) away from the flow and b) into the flow

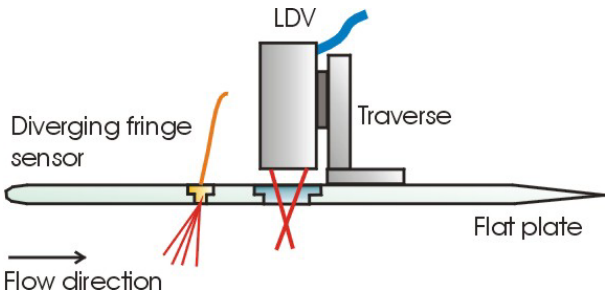

Figure 6. Schematic of the test section with the flat plate.

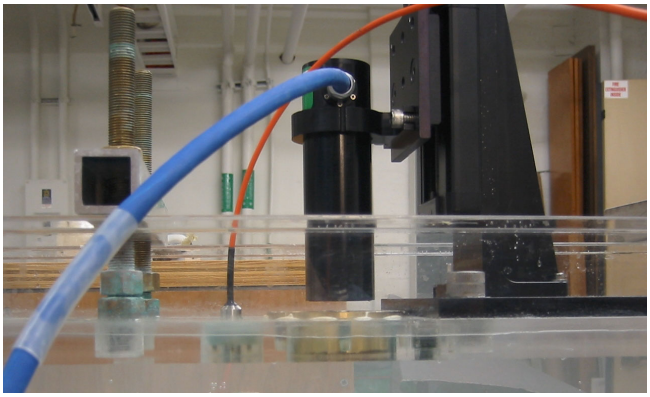

Figure 7 Photograph of the experimental setup for the flat plate experiment.

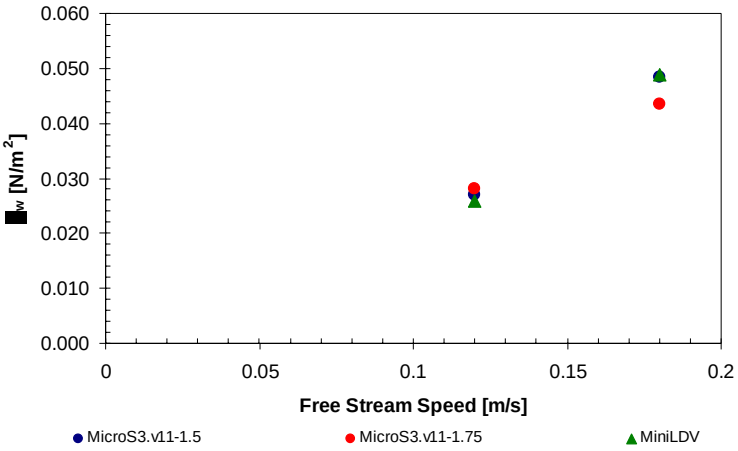

Figure 8 Results of the wall shear stress measurements obtained with the LDV and two versions of the Diverging Doppler Fringe sensor.

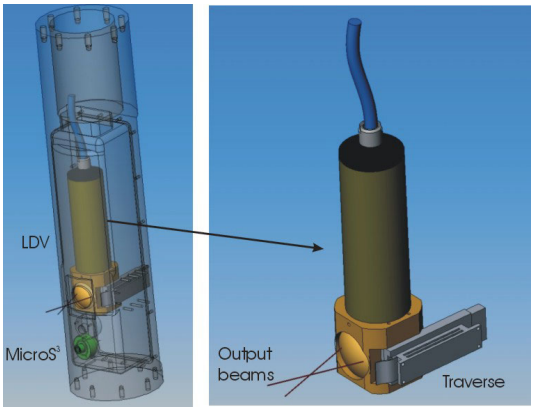

Figure 9 Mechanical design of the instrumented cylinder.

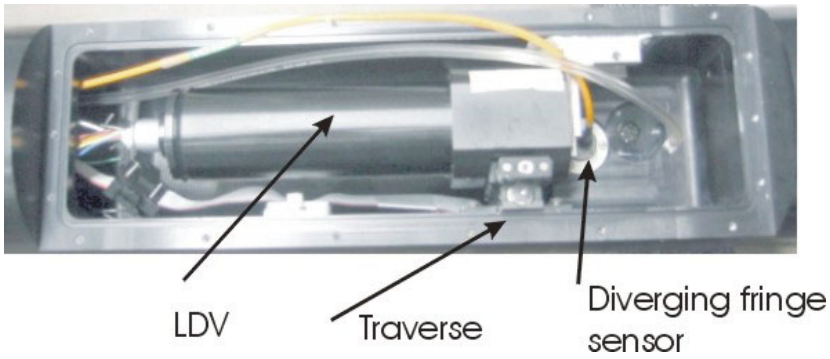

Figure 10 Photograph of the instrumented cylinder.

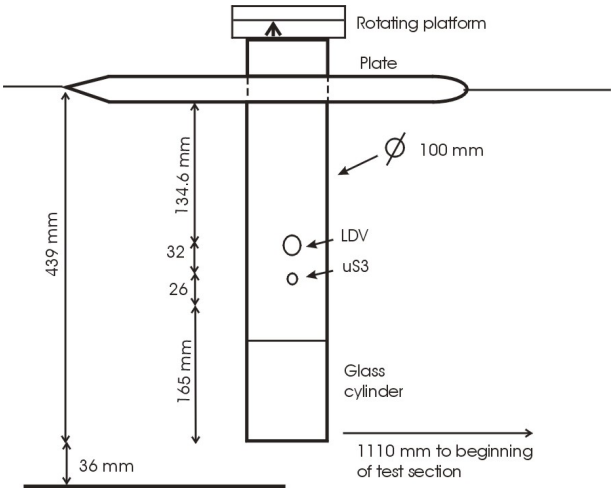

Figure 11 Position and dimensions of the cylinder in the Noah tunnel

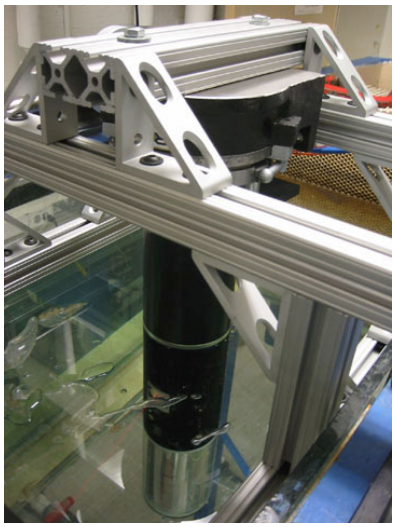

Figure 12 Photograph of the cylinder installed in the Noah tunnel

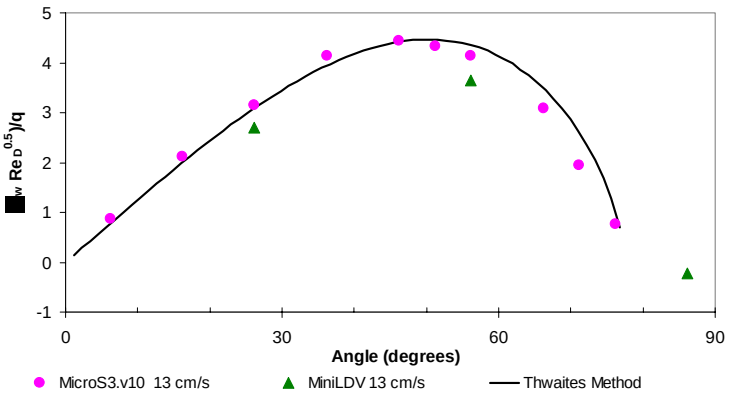

Figure 13 Normalized shear stress calculated from the boundary layer surveys and from the Diverging Fringe Doppler sensor measurements in the Noah tunnel.

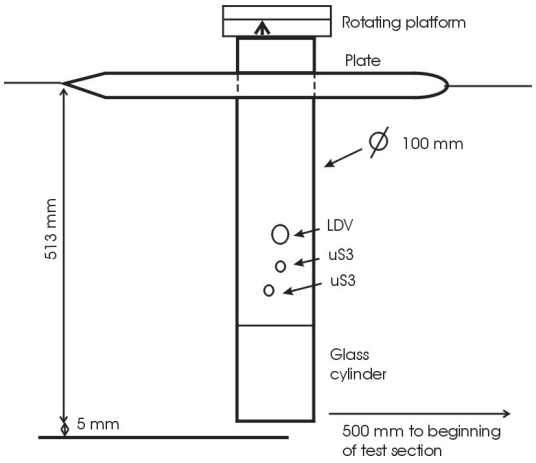

Figure 14 Position and dimensions of the cylinder in the Large Free Surface Tunnel

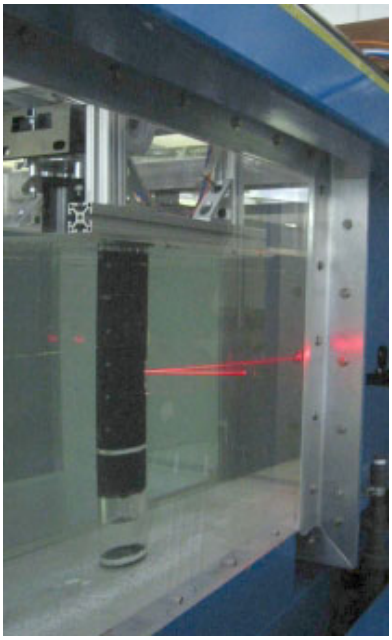

Figure 15 Photograph of the cylinder installed in the Large Free Surface tunnel

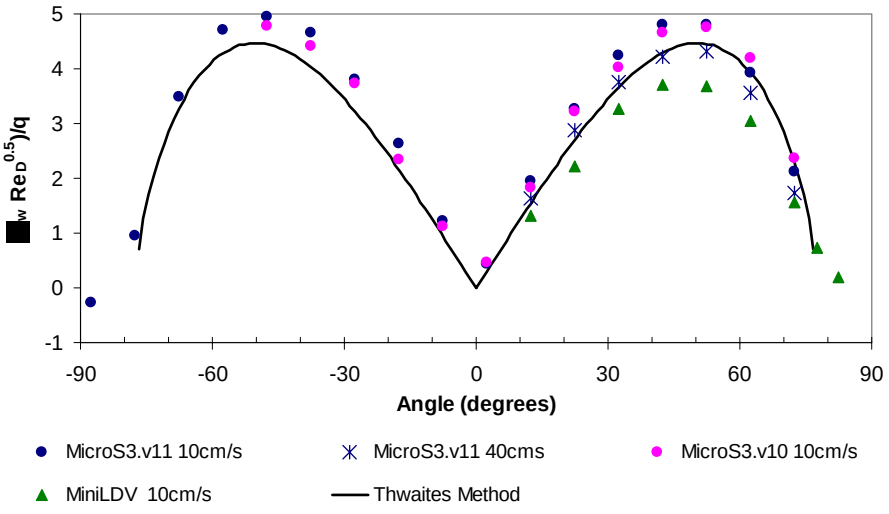

Figure 16 Normalized shear stress values calculated from the boundary layer surveys and from the Diverging Fringe Doppler sensor measurements in the Large Free Surface Tunnel.

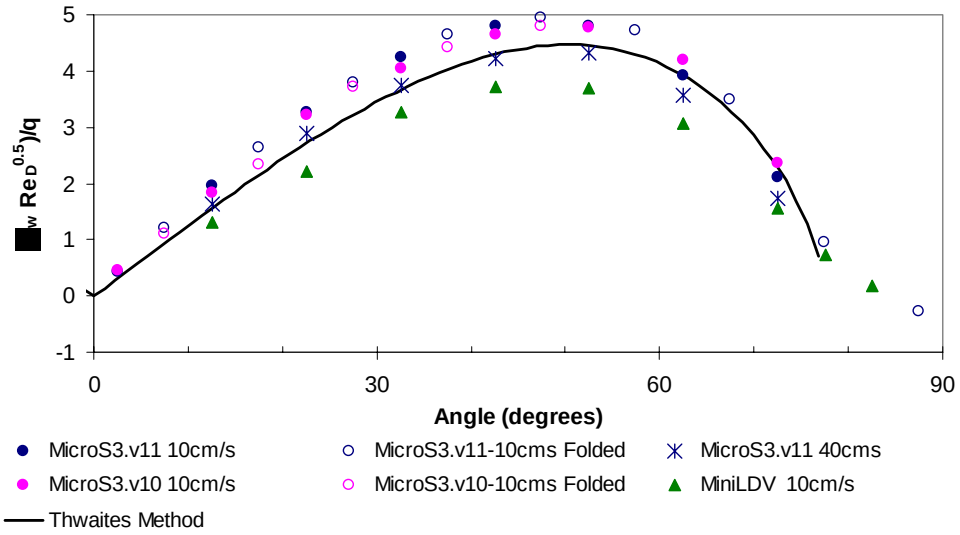

Figure 17 Shear stress values obtained during the Large Free Surface Tunnel tests, folded on a single axis.

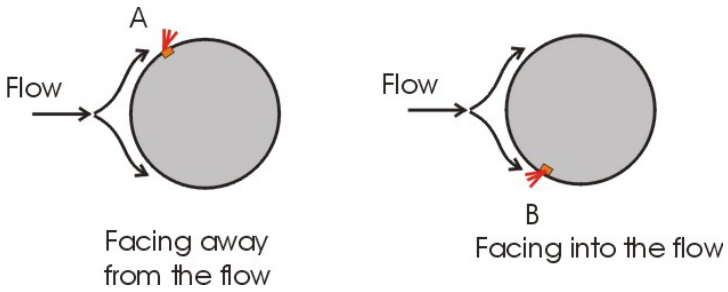

Figure 18 Sketch of the sensor position to test the sensor directionality

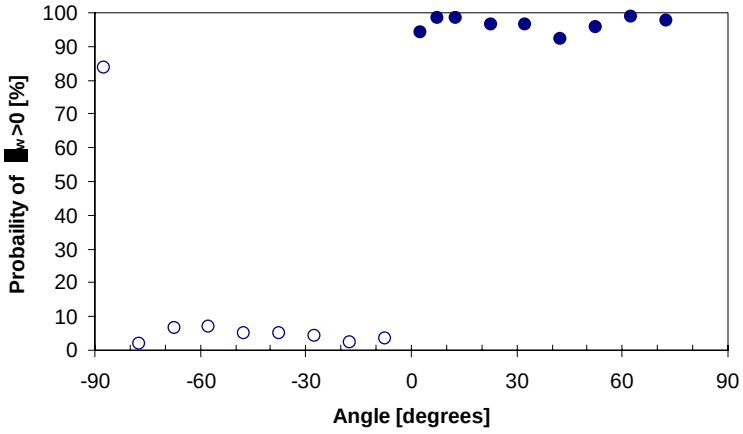

Figure 19 Probability of determining flow direction for fringes facing into the flow (frequency increase) and facing away from the flow (frequency decrease)